Einstein-Podolsky-Rosen paradox implies a minimum achievable temperature

David M. Rogers
Department of Chemistry, University of South Florida, Tampa, Florida 33620, USA
(Received 25 February 2016; revised manuscript received 21 July 2016; published 25 January 2017)

This work examines the thermodynamic consequences of the repeated partial projection model for coupling a quantum system to an arbitrary series of environments under feedback control. This paper provides observational definitions of heat and work that can be realized in current laboratory setups. In contrast to other definitions, it uses only properties of the environment and the measurement outcomes, avoiding references to the "measurement" of the central system's state in any basis. These definitions are consistent with the usual laws of thermodynamics at all temperatures, while never requiring complete projective measurement of the entire system. It is shown that the back action of measurement must be counted as work rather than heat to satisfy the second law. Comparisons are made to quantum jump (unravelling) and transition-probability based definitions, many of which appear as particular limits of the present model. These limits show that our total entropy production is a lower bound on traditional definitions of heat that trace out the measurement device. Examining the master equation approximation to the process at finite measurement rates, we show that most interactions with the environment make the system unable to reach absolute zero. We give an explicit formula for the minimum temperature achievable in repeatedly measured quantum systems. The phenomenon of minimum temperature offers an explanation of recent experiments aimed at testing fluctuation theorems in the quantum realm and places a fundamental purity limit on quantum computers.

DOI: 10.1103/PhysRevE.95.012149

I. INTRODUCTION

A version of the EPR paradox prevents simultaneously doing work on a quantum system and knowing how much work has been done. A system can do work on its environment only if the two have a nonzero interaction energy. During interaction, the two become entangled, leading to a superposition of different possible values for the work. According to quantum mechanics, measuring the energy of either system removes correlations so that the interaction energy becomes exactly zero [1]. Therefore either the system-environment interaction is zero or the work is unknown.

We argue that this paradox presents the central difficulty in applying fluctuation theorems (FT) and work relations to quantum systems. It is a restatement of the energy-time uncertainty principle, and therefore manifests whenever energy measurements are preformed on nontrivial quantum systems.

One hundred years ago, Einstein presented a first-order rate hypothesis concerning the rate of energy exchange between a molecular system and a reservoir of photons [2]. Under this hypothesis, the transition between states with known molecular energy levels by emission and absorption of discrete photons can be shown to bring about thermal equilibrium for all parties: the photons, the molecular energy levels, and the particle velocities. This semiclassical picture provided a clear, consistent, and straightforward picture for the time evolution of coupled quantum systems. Nevertheless, the argument must have appeared unsatisfactory at the time because it only provided a statistical, rather than an exact, mechanical description of the dynamics.

Many years later, Einstein, Podolsky, and Rosen published the famous EPR paradox [3,4]. The paradox states that, before any measurement is made, neither position nor velocity exist as real physical quantities for a pair of entangled particles. Either of the two choices can be "made real" only by performing a measurement. The consequence for energy exchange processes follows directly. For a two-state system entangled with a field, no definite separation of energy between the molecule and the field exists before any measurement is made.

Recent works on quantum fluctuation theorems confront this difficulty in a variety of ways. One of the most prominent is the quantum jump method based on a stochastic unravelling of Lindblad equation [5,6]. It replaces a dissipative quantum master equation with an ensemble of trajectories containing periodic jumps due to measurement [7]. In that setup, the jump process represents dissipation, so heat is defined as any energy change in the system due to the jumps. Other changes in energy, caused by varying the Hamiltonian in time, are counted as work. Fluctuation theorems for this process are based on the detailed balance condition for jumps due to the reservoir, avoiding most issues with defining a work measurement. Application of the jump process for a Jaynes-Cummings system showed that the fluctuation theorem for work is followed exactly when the the coupling uses the rotating wave approximation [8]. However, that approximation removes the essential difficulty with the energy-time uncertainty relation [9].

The work of Venkatesh [10] on general coupling Hamiltonians shows that regular, projective measurement of worklike quantities based on the system alone (such as the time derivative of the Hamiltonian expectation) generally leads to "qualitatively different statistics from the [two energy measurement] definition of work and generally fail to satisfy the fluctuation relations of Crooks and Jarzynski."

Another major approach is to model the environment's action as a series of generic quantum maps. A physical interpretation as a two-measurement process accomplishing feedback control was given by Funo [11]. There, an initial projection provides classical information that is used to choose a Hamiltonian to evolve the system for a final measurement.

That work showed that the transition probabilities in the process obey an integral fluctuation theorem. Although the interpretation relied on a final measurement of the system's energy, it provided one of the first examples for the entropic consequences of measurement back action [12].

Recent work on the statistics of the transition process for general quantum maps showed that the canonical fluctuation theorems hold as long as the maps can be decomposed into transitions between stationary states of the dynamics [13]. This agrees with other works showing the importance of stationary states in computing entropy changes from quantum master equations [14]. In other words, the essential difficulties with the quantum case come from differences between the basis in which the dynamics is carried out and that in which the measurement is done.

In contrast to these approaches, the present work starts from a physically realizable measurement process and shows that work and heat can be defined independently—without recourse to stationary states of the central system. By doing so, it arrives at a clear picture of the back action, and a minimum temperature argument. It also builds a quantum parallel to the measurement-based definition of work and heat for classical nonequilibrium systems laid out in Ref. [15]. There, the transition probability ratio is shown to be equivalent to a physical separation of random and deterministic forces. Although no fluctuation theorem can be shown in general, our expressions reduce to well-known limits. In particular, for weak coupling the interaction commutes with the total uncoupled energy, $\hat{H}_A + \hat{H}_B$, and a fluctuation theorem such as the one in Ref. [13] applies.

We consider a combination of system and reservoir with time-independent joint Hamiltonian,

$$\hat{H} = \hat{H}_A + \hat{H}_B + \gamma \hat{H}_{AB}. \tag{1}$$

The coupling Hamiltonian should not be able to simply shift an energy level of either system, which requires $\mathrm{Tr}_A\,[f(\hat{H}_A)\hat{H}_{AB}] = 0$ and $\mathrm{Tr}_B\,[f(\hat{H}_B)\hat{H}_{AB}] = 0$, for arbitrary functions, f. A simple generalization discussed later is to waive the first constraint, but this is not investigated here. Time dependence comes in by the choice of $\hat{H}_{AB}$ and the initial state ρ_B at the start of each measurement interval.

There have been many definitions proposed for heat and work in quantum systems. These fall roughly into three categories: the near-equilibrium limit, experimental work-based definitions, and mathematical definitions based on information theory.

The near-equilibrium limit is one of the earliest models, and is based on the weak-coupling limit of a system interacting with a quantum energy reservoir at a set temperature over long time intervals. That model is probably the only general one derivable from first principles where it can be proven that every system will eventually relax to a canonical equilibrium distribution with the same temperature as the reservoir [16]. The essential step is taking the Van Hove limit, where the system-reservoir interaction energy scale γ goes to zero (weak coupling) with constant probability for energy-conserving transitions [which scale as $\gamma^2/(\hbar^2\lambda)$]. In this limit, the only allowed transitions are those that conserve the uncoupled energy, $\hat{H}_A + \hat{H}_B$. The dynamics then becomes a process obeying detailed balance for hopping between energy levels of the system's Hamiltonian $\hat{H}_A$. States with energy superpositions can mix, but eventually decay to zero probability as long as the environment can couple to every system energy level.

Adding an effective time-dependent Hamiltonian $\hat{H}_A^{\mathrm{eff}}(t)$ onto this picture and assuming very long-time scales provides the following definitions of heat and work [17]:

$$\begin{aligned} \dot{Q}_{\mathrm{eff}} &= \mathrm{Tr}\left[\hat{H}_A^{\mathrm{eff}}(t)\dot{\rho}\right], \\ \dot{W}_{\mathrm{eff}} &= \mathrm{Tr}\left[\frac{\partial \hat{H}_A^{\mathrm{eff}}(t)}{\partial t}\rho\right], \end{aligned} \tag{2}$$

where $\dot{F} = dF/dt$ denotes the time derivative of F according to the dynamics, and $e^{-\beta \hat{H}_A^{\mathrm{eff}}(t)}$ must be the stationary state of the time evolution used. Note that to match the dynamics of a coupled system, $\hat{H}_A^{\mathrm{eff}}(t)$ must be a predefined function of t satisfying [see Eq. (14)]

$$\mathrm{Tr}\left[\hat{H}_A^{\mathrm{eff}}(t)\,\mathrm{Tr}_B[\rho_{AB}]\right] = \mathrm{Tr}[(\hat{H}_A + \gamma \hat{H}_{AB})\rho_{AB}]. \tag{3}$$

Work and heat defined by Eq. (2) have been used extensively to study quantum heat engines [14,17–24]. For this definition, it is possible to prove convexity [16], and positivity of $\dot{S}_{\mathrm{tot}} = \dot{S}_A - \beta \dot{Q}_{\mathrm{eff}}$ [17]. Statistical fluctuations of heat and work have also been investigated [7,11,13,25]. These first applications have demonstrated some of the interesting properties of quantum systems, but encounter conceptual difficulties when applied to dynamics that does not follow the instantaneous eigenstates of $H_A^{\mathrm{eff}}(t)$ [10,12,14].

The paradox described in this work shows why moving away from eigenstates is so difficult. The small-coupling, slow-process limit under which Eq. (2) applies also amounts to an assumption that the system-environment pair is continually being projected into states with known effective energy. Its validity in deriving quantum fluctuation theorems relies on this particular choice of basis.

Entropy can also be defined thermodynamically by analyzing physical processes taking an initial state to a final state. One of the simplest results using the thermodynamic approach is that even quantum processes obey a fluctuation theorem for exchanges of (heat) energy between system and environment when each transition conserves energy and there is no external driving force [26]. On averaging, this agrees with the common experimental definition of heat production as the free energy change of two reservoirs set up to dissipate energy by a quantum contact that allows monitoring the energy exchange process [27–30]. Semiclassical trajectories have also been investigated as a means to show that postulated expressions for quantum work go over to the classical definition in the high-temperature or small-$\hbar$ limit [31].

Other works in this category consider a process where the system's energy is measured at the start and end of a time-dependent driving process. It is then easy to show that the statistics of the energy change give a quantum version of the Jarzynski equality for the free energy difference [32,33]. More general results are difficult owing to the fact that, for coupled systems, quantum transitions that do not conserve uncoupled energy are possible, giving rise to the paradox motivating this work.

There have also been many mathematically based definitions of entropy production for open quantum systems.

The primary goal of a mathematical definition is to quantify the information contained in a quantum state [34]. It is well known that preparation of a more ordered system state from a less ordered one requires heat release proportional to the information entropy difference [35,36]. From this perspective, information is more fundamental than measured heats, because it represents a lower bound on any physical process that could accomplish this transformation. A maximum work could be found from such a definition using energy conservation. However, the disadvantage of a mathematical definition is that it cannot be used to construct a physical transformation process obeying these bounds.

Most of the bounds on mathematical entropy production are proven with the help of the Klein inequality stating that relative entropy between two density matrices must be positive [37]. There are, in addition, many connections with communication and measure theory that provide approximations to the relative entropy [34,38].

One particular class of mathematical definitions that has received special attention is the relative entropy,

$$\begin{aligned} S(\rho|\rho^{\text{inst}}) &= \text{Tr}[\rho\ln\rho - \rho\ln\rho^{\text{inst}}] \\ &= \beta[F(t) - F^{(\text{eq})}], \end{aligned} \tag{4}$$

between an arbitrary density matrix and an "instantaneous equilibrium" state,

$$\rho^{\text{inst}} = \exp\left[-\beta\hat{H}^{\text{eff}}(t)\right]/Z^{\text{eff}}(\beta,t). \tag{5}$$

This definition is closely related to the physical process of measuring the system's energy at the start and end of a process. Several notable results have been proven in those works, including work relations and integrated fluctuation theorems [11,13,32,39,40] as well as useful upper and lower bounds [7,41]. The present work is distinguished from these mathematical definitions because it completely removes the requirement for defining or using an instantaneous equilibrium distribution of the central system or directly measuring the central system at all.

One of the primary motivations for this work has been to derive a firm theoretical foundation for analyzing time sequences of measurements in hopes of better understanding the role of the environment in decoherence [42–51]. The present paper provides a way of understanding the gap between the Lindblad operators describing the quantum master equation and the physical processes responsible for decoherence. Rather than unravelling the Lindblad equation [6], we choose a physical process and show how a Lindblad equation emerges. The result also provides an alternative continuous time, Monte Carlo method for wave-function evolution [52,53] without using the dissipation operator associated with the Lindblad master equation.

Another outcome has been finding a likely explanation for the anomalous temperature of Utsumi *et al.* [27,28]. Those experiments attempted to test the classical fluctuation theorems for electron transport through a quantum point contact, and found that the effective temperature of 1.37 K (derived by fitting the slope of the transport odds ratio, $\ln p_{\text{fwd}}/p_{\text{rev}}$ to the fluctuation theorem) was much higher than the electron temperature of 130–300 mK. Trying to lower the temperature further below 1.37 K showed minimal changes in the slope, indicating a minimum temperature had been reached.

Sections II and III present a repeated measurement process, and show that it allows for a physical definition of heat and work that occurs between successive measurements. Measurements are only performed on the interacting reservoir, and (because of entanglement) cause instantaneous projection of the central system according to the standard rules of quantum mechanics. In this way, it is not required to define a temperature for the central system. Because the central system is generally out of equilibrium, the concept of equilibrium is applied only to the environmental interactions.

Section IV proves the Clausius form of the second law for the new definitions. Numerical results on simulations of atom-cavity systems are presented in Sec. V. Specifically, we perform Monte Carlo simulations of trajectories of the time-dependent density matrix during relaxation to equilibrium. The system is a simplified micromaser (a dissipation-free single-mode optical cavity) started in its first excited state, and the reservoir is a stream of thermal two-level atoms. Since the propagator is non-Markovian, we also derive the Markovian approximation in the Linblad representation. The heat and work performed on the system by the passing atoms is compared between the two methods. Finally, in Sec. VI, we show that continuous finite interaction with the reservoir causes an effective increase in the "temperature" of the system's steady state. Although surprising, the measurement rate is unavoidable in the theory as it is the exact parameter controlling broadening of spectral lines [54]. Effects from the minimum achievable temperature will be seen when all of the following conditions are met: (i) the reservoir temperature is less than the system's first excitation energy, (ii) the measurement rate is on the order of this excitation energy, and (iii) the commutator, $[\hat{H},\hat{H}_{AB}]$, is nonzero.

II. REPEATED MEASUREMENT PROCESS

To study the action of continual environmental measurement on part of a quantum system, we propose the following process (Fig. 1):

(1) Let $|\psi\rangle$ represent a general wave function of the central system at time t_j.

(2) At time t_j, the central system is coupled to a measurement device whose state $|n\rangle$ is chosen at random from a starting distribution $\rho_B(t_j)$ that is diagonal in the measurement Hamiltonian, so that $\hat{H}_B|n\rangle = \hbar\omega_{B,n}|n\rangle$ [Fig. 1(a)],

$$|\psi\rangle \to |\psi\rangle \otimes |n\rangle. \tag{6}$$

(3) The joint system is evolved forward using the coupled Hamiltonian, $\hat{U}(t) = e^{-it\hat{H}/\hbar}$ until the next measurement time $t_{j+1} = t_j + t$ [Figs. 1(b) and 1(c)]. Our numerical calculations assume a Poisson measurement process with rate λ, so that t has an exponential distribution,

$$|\psi,n\rangle \to \hat{U}(t)|\psi,n\rangle. \tag{7}$$

(4) The state of the measurement device is "measured" via projection into one of its uncoupled energy eigenstates, $|m\rangle$ at

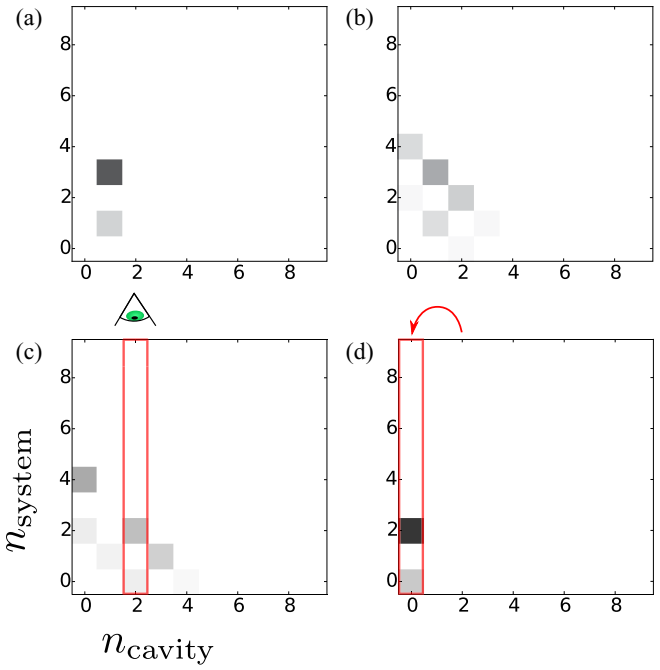

FIG. 1. Schematic of the repeated measurement process. (a)–(c) Exact evolution of the coupled system + reservoir from an uncoupled state quickly leads to an entangled state. (c) Measuring the reservoir energy selects a subsample of the system, removing coherences. (d) Replacing the reservoir state with a thermal sample results in heat and work output. The thermal nature of the environment is responsible for dissipation.

time t_{j+1} [Fig. 1(c)],

$$\hat{U}(t)|\psi,n\rangle \to |\psi'\rangle = \frac{\langle m|\hat{U}(t)|\psi,n\rangle}{\sqrt{p_m}}. \tag{8}$$

This causes the system to undergo a quantum jump with probability $p_m = |\langle m|U(t)|\psi,n\rangle|^2$ [Fig. 1(d)]. The resulting state, $|\psi'\rangle$, is sent as input to step 1.

When expressed in density matrix notation, steps 4, 1, and 2 combine together to form the "purification" superoperator of Spohn and Lebowitz [16],

$$\hat{P}\rho_{AB}(t) = [\mathrm{Tr}_B\, \rho_{AB}(t)] \otimes \rho_B(0). \tag{9}$$

Every time this operation is performed, the memory of the environmental system is destroyed, all system-environment superposition is removed, and $\langle \hat{H}_{AB}\rangle$ necessarily becomes zero as explained following Eq. (1). To make use of the information on the measured state of B, this work treats "measurement" (step 4) and "thermalization" (step 2) as separate steps.

For studying the thermalization process, it suffices to use a constant, thermal equilibrium distribution for $\rho_B(t_j)$,

$$\rho_B^{\text{eq}}(\beta) = e^{-\beta \hat{H}_B}/Z_B(\beta). \tag{10}$$

In many experimental cases, $\rho_B(t_j)$ represents a specially prepared protocol to drive the system toward a desired state. Since our calculations are for the case where the environment is not time dependent, we will use $\rho_B(0) = \rho_B(t_j)$ interchangeably.

The operation of measurement disconnects the two systems, and, more importantly, makes the energy of the reservoir system correspond to a physical observable. A complete accounting for heat in quantum mechanics can be made using only these measurements on ancillary systems, rather than the central, A, system. The thermodynamics based on this accounting allows the central system to retain most of its quantum character, while at the same time deriving the traditional, operational relationships between heat and work.

Although the analysis below is phrased in terms of density matrices, that view is equivalent to carrying out this process many times with individual wave functions. Specifically, if $\rho_A(t_j) = \sum_k p_k|\psi_k\rangle\langle\psi_k|$ is composed of any number of pure states [55], the final density matrix at time t_{j+1} is a linear function of ρ_A and hence of each $|\psi_k\rangle\langle\psi_k|$. Carrying out the process on individual wave functions thus allows an extra degree of choice in how to compose $\rho_A(t_j)$, the use of which does not alter any of the results.

This process is a repeatable version of the measurement and feedback control process studied in Ref. [11], gives a discrete-time version of quantum state diffusion [5], and fits into the general quantum map scheme of Ref. [13]. Nevertheless, our analysis finds different results because our thermodynamic interpretation of the environment and measuring device allows the reservoir to preform work in addition to exchanging heat.

III. THERMODYNAMICS OF REPEATED MEASUREMENT

In order for heat and work to have an unambiguous physical meaning, they must be represented by the outcome of some measurement. Figure 2 presents the energies for each operation applied to a system and its reservoir over the course of a measurement interval in Fig. 1. This section assumes $t_j = 0$ without loss of generality. Initially (in step 2), the density matrix begins as a tensor product, uncoupled from the reservoir, which has a known starting distribution, $\rho_B(0)$. However, for a coupled system and measurement device, time evolution leads to entanglement. At the time of the next measurement, the entanglement is projected out, so it is again

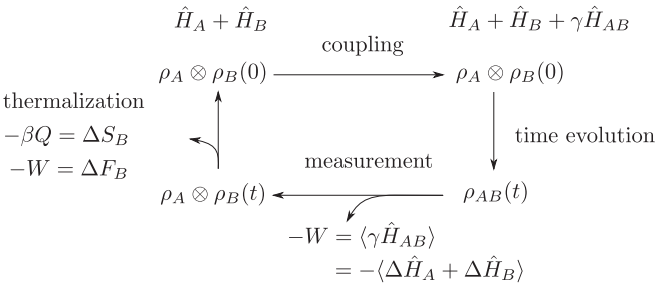

FIG. 2. Work and heat of the intermittently measured quantum system. On the left, the system (A) and reservoir (B) Hamiltonians are uncoupled. Coupling (step 2 in the process of Sec. II) does not initially change their energy, since diagonal elements of $\hat{H}_{AB}$ are zero. During time evolution (step 3), the total energy is conserved, leading $\langle\hat{H}_{AB}\rangle$ and $\langle\hat{H}_A + \hat{H}_B\rangle$ to oscillate. Measurement (step 4) projects back into an uncoupled state, requiring work $-\langle\gamma\hat{H}_{AB}\rangle$. $\rho_A \otimes \rho_B(t)$ is schematic in this figure, as discussed in the text surrounding Eqs. (25) and (28). Finally, thermalization of the reservoir removes accumulated heat, while exporting all work to the environment.

permissible to refer to the properties of the A and B systems separately.

After a measurement, the total energy of the system-reservoir pair will have changed from $\langle \hat{H}_A + \hat{H}_B + \gamma \hat{H}_{AB} \rangle$ to $\langle \hat{H}_A + \hat{H}_B \rangle$. The amount of energy that must be added to measure the system-reservoir pair at any point in time is therefore $-\gamma \langle \hat{H}_{AB} \rangle$.

This step is responsible for the measurement "back action," and the violation of the FT for general quantum dynamics. Strictly speaking, this measurement energy does not correspond to an element of physical reality. Nevertheless, the starting and ending $\hat{H}_A$, $\hat{H}_B$ are conserved quantities under the uncoupled time evolution, and so the energy of the measurement step can be objectively defined in an indirect way.

This instantaneous measurement of the reservoir simulates the physical situation where an excitation in the reservoir leaks out into the environment. After this happens, the information it carried is available to the environment, causing traditional collapse of the system-reservoir pair.

To complete the reset from step 4 back to step 1, the reservoir degree of freedom must be replaced with a new sample from its input ensemble. For the micromaser, this replacement is accomplished spatially by passing separate atoms (B) through a cavity, one at a time.

On average, the system should output a "hot" $\rho_B(t)$, which the environment will need to cool back down to $\rho_B(0)$. Using the methods of ordinary thermodynamics [17,19,22], we can calculate the minimum heat and maximum work for transformation of $\rho_B(t)$ back to $\rho_B(0)$ via an isothermal, quasistatic process at the set temperature of the reservoir,

$$\begin{aligned} \beta Q &= -\operatorname{Tr}[\rho_B(0)\ln\rho_B(0)] + \operatorname{Tr}[\rho_B(t)\ln\rho_B(t)] \\ &= -\Delta S_B, \end{aligned} \tag{11}$$

$$\begin{aligned} W_{\text{therm}} &= \operatorname{Tr}\left[[\rho_B(0) - \rho_B(t)]\hat{H}_B\right] + \Delta S_B/\beta \\ &= -\Delta F_B, \end{aligned} \tag{12}$$

$$\begin{aligned} W &= W_{\text{therm}} + \Delta H_A + \Delta H_B \\ &= \Delta H_A - Q. \end{aligned} \tag{13}$$

These signs of these quantities are defined as the energy added to the system, while $\Delta X \equiv \langle \hat{X} \rangle_{\text{final}} - \langle \hat{X} \rangle_{\text{initial}}$ represents the total change in $\hat{X}$ during evolution from one measurement time to the next.

In this work, T always refers to the externally set temperature of the reservoir system. The temperature of the reservoir, used in defining $\beta = 1/k_B T$ above, is entirely related to the conditions under which the reservoir states are prepared. It can be different for each measurement interval.

Note that when a thermal equilibrium distribution is used for the reservoir [Eq. (10)], the reservoir dissipates energy from the system. Since it always begins in a state of minimum free energy, the reservoir always recovers work from the system as well, since $-W_{\text{therm}}$ is always positive by the non-negativity of Eq. (4). This makes sense when the central system is relaxing from an initial excited state. When the central system is at equilibrium, the second law is saved (Sec. IV) by including the work done during the measurement step.

A. Caution on using a time-dependent Hamiltonian

The assumption of a time-dependent Hamiltonian for the system leads to an ambiguity on the scale of the measurement back-action [10–12]. This presentation does not follow the traditional route of assuming a time-dependent Hamiltonian for the central system. The assumption of a time-dependent Hamiltonian is awkward to work with in this context because it sidesteps the measurement paradox. Instead, it assumes the existence of a joint system wherein the dynamics for subsystem A is given exactly by $\dot{\rho}_A(t) = -\frac{i}{\hbar}[\hat{H}_A^{\text{eff}}(t), \rho_A(t)]$.

The complete physical system plus environment must have a conserved energy function. This matches the dynamics,

$$\dot{\rho}_A(t) = -\frac{i}{\hbar} \operatorname{Tr}_B[\hat{H}_A + \hat{H}_B + \gamma \hat{H}_{AB}, \rho_{AB}(t)], \tag{14}$$

exactly when Eq. (3) holds.

In classical mechanics, such a function can be formally constructed by adding an ancillary degree of freedom y that moves linearly with time, $y(t) = t$. The potential energy function,

$$V(x,y) = V(x) + V^{\text{int}}(x,y) - \int_0^y \frac{\partial V^{\text{int}}(x_{\text{ref}}(t),t)}{\partial t} dt, \tag{15}$$

is defined using the known trajectory for $x_{\text{ref}}(t)$ under the desired Hamiltonian, $H(x,t)$, so that y experiences no net force. Alternatively, y can be considered to be infinitely massive.

When translated to quantum mechanics, neither of these last two methods avoids the Heisenberg uncertainty principle [31,56]. An intuitive argument can be based on $\langle \Delta p \rangle \langle \Delta x \rangle \geqslant \frac{\hbar}{2}$. In both cases, the work done by the system on the reservoir is $\frac{\partial V^{\text{int}}(x,y)}{\partial dy} dy$, and contributes directly to the change in momentum of y. The y coordinate was constructed to move linearly in time, and hence measures the "time" of interaction. Using these translations from momentum change and position to work and time provides $\langle \Delta p_y \rangle \langle \Delta y \rangle \simeq \langle \Delta_t V(x,t) \rangle \langle \Delta t \rangle$.

Although the definitions of heat and work in Eq. (2) can be shown to be mathematically consistent with the laws of thermodynamics, they require infinitesimally slow time evolution under the Markov assumption and constant comparison to a steady-state distribution [13,14,17]. The present method is valid under a much less restrictive set of assumptions. In particular, it allows arbitrary time evolution, and only makes use of the equilibrium properties of the B system, not the central A system. The present set of definitions is also directly connected to the experimental measurement process.

Strong-coupling schemes define a time-dependent $\hat{H}$, which groups the central system together with some aspects of the reservoir. In the present framework, it is easy to allow $\hat{H}_B$ and $\hat{H}_{AB} = \hat{H}'_{AB} + \hat{H}'_A$ to be different for each measurement interval (encompassing even non-Markovian dynamical schemes [45,57,58]). In this case, the analysis above mostly carries through, with the exception that, since $\langle f(\hat{H}_A)\hat{H}_{AB} \rangle \neq 0$, an extra amount of energy is added during coupling, but not removed during measurement. This extra energy contributes to the work done on the system according to Eq. (2). However, the connection to heat found here is very different because, as the next subsection shows, the

definition of heat in Eq. (2) requires that the reservoir be near equilibrium. The comparison presented here is conceptually simpler because energy stored in the system cannot be instantaneously altered by an external source.

For a specific example, consider the energy exchange process taking place between a nuclear spin and its environment in an NMR spin-relaxation experiment [23]. In order to represent stored energy, the Hamiltonian of the atom can be defined with respect to some static field, $\hat{H}'_A = \frac{\hbar\omega_0}{2}\sigma_z$. Rather than varying the field strength (ω_0) directly, changing the atomic state from its initial equilibrium can be brought about with an interaction Hamiltonian, $\hat{H}'_{AB}$, such as the Rabi model studied here. The work can be added over each time interval to give

$$\int_0^t dt'\ W(t') = \frac{\hbar\omega_0}{2}\,\mathrm{Tr}\{\sigma_z[\rho_A(t) - \rho_A(0)]\} - \int_0^t dt'\ Q(t'). \tag{16}$$

The heat release can be analyzed using either of the methods in the next section (Sec. III B). Assuming the minimum heat release leads to $\int_0^t dt'\beta(t')Q(t') = S_A(t) - S_A(0)$, in agreement with the rules of equilibrium thermostatics. Alternately, in the limit where the B system always begins at thermal equilibrium and moves infinitesimally slowly between each measurement interval, Eq. (2) is recovered, giving $W(t) = 0$. The key point is that this model separates the system and environment in such a way that changes in the environment cannot instantaneously change the energy stored in the system.

B. Comparison to common approximations for the heat evolution

The heat generated in the process of Figs. 1 and 2 comes directly from the entropy change of the measurement system B. Most analyses ignore the measurement system, making this result difficult to compare with others in the literature. This section presents two simple methods for calculating ΔS_B from quantities available in other methods.

First, assuming the time dependence of $\rho_A(t)$ is known, a lower bound on the heat emitted can be derived from the state function, $S_A(t) = -\,\mathrm{Tr}\,[\rho_A \ln \rho_A]$. Over each time interval, $\Delta S_A + \Delta S_B \geqslant 0$, so the total heat added obeys the inequality,

$$\Delta Q(t) = -\Delta S_B/\beta \leqslant \Delta S_A/\beta. \tag{17}$$

Assuming the minimum required heat release leads to a prediction of the quasistatic heat evolution,

$$\int_0^t \frac{dQ(t')}{dt'}dt' \leqslant \int_0^t dS_A(t')/\beta(t')\,dt'. \tag{18}$$

This is exactly the result of equilibrium quantum thermodynamics, valid for arbitrary processes, $\rho_A(t)$.

Second, if the B system always begins in thermal equilibrium, $\rho_B(0) = \rho_B^{(\beta)}$, and the change in occupation probability for each energy level [$\Delta\,\mathrm{diag}(\rho_B)$] over a measurement interval is small, then we can directly use the expansion [16]

$$\delta S_B = -\sum_j \delta p_j \ln p_j. \tag{19}$$

This is helpful because in Fig. 2, the entropy of the B system is always calculated in the energy basis of B. Substituting the canonical equilibrium distribution,

$$\delta Q = -\sum_j \delta p_j E_j = -\delta H_B. \tag{20}$$

Equations (19) and (20) apply whenever $\rho_B(0)$ is a canonical distribution and the change in ρ_B is small over an interval.

In the Van Hove limit (see Appendix B), energy is conserved between the A and B systems. Because of energy conservation, the heat evolution of Eq. (20) is exactly the well-known result of Eq. (2) in this case. We have therefore proven that our scheme is bounded by the von Neumann entropy and that it reduces to the standard definitions in the weak-coupling limit.

IV. THERMODYNAMIC CONSISTENCY

For the definitions of work and heat given above to be correct, they must meet two requirements. In order to satisfy the first law, the total energy gain at each step must equal the heat plus work from the environment. This is true by construction because the total energy change over each cycle is just $\langle\Delta\hat{H}_A\rangle$. Next, in satisfaction of the second law, the present section will show that there can only be a net heat release over any process returning to its initial thermodynamic state. Since Q has been defined as heat input to the system, this means

$$\oint Q \leqslant 0. \tag{21}$$

There is a fundamental open question as to whether the energy change caused by the measurement process should be classified as heat or work. Counting it as heat asserts that it is spread throughout the environment in an unrecoverable way. Conversely, counting it as work asserts that measurement can only be brought about by choosing to apply a stored force over a distance. In the cycle of Fig. 2, it is classified as work, because this is the only assignment consistent with thermodynamics.

Counting $\langle\gamma\hat{H}_{AB}\rangle$ as heat leads to a systematic violation of the second law, as is now shown. Over a thermodynamic cycle (many repetitions of the measurement cycle of Fig. 2), ρ_A must eventually return to its initial state. Therefore $\oint\langle\Delta H_A\rangle$ drops out when integrating the quantity

$$R = \langle\Delta H_A\rangle + \langle\Delta H_B\rangle - \Delta S_B/\beta \tag{22}$$

to leave

$$\oint R = \oint\langle\Delta H_B\rangle - \Delta S_B/\beta. \tag{23}$$

If the B subsystem starts each interval in thermal equilibrium [Eq. (10)], this is the free energy difference used in Eq. (4). The Klein inequality then proves the *positivity* of each contribution to Eq. (23). Therefore, over a cyclic process, $\oint R \geqslant 0$.

A thermodynamically sound definition is found when counting as part of Q only the entropy change of the reservoir. Heat comes into this model because the environment is responsible for transforming $\rho_B(t)$ back into $\rho_B(0)$. Using a hypothetical quasistatic, isothermal process to achieve this will require adding a heat, $Q = [S_B(0) - S_B(t)]/\beta = -\Delta S_B$.

We now show that $\oint \Delta S_B \geqslant 0$ by considering entropy changes for the A-B system jointly. At the starting point of each measurement cycle, the two systems are

decorrelated [38],

$$S[\rho_A(0)\otimes\rho_B(0)] = S_A(0) + S_B(0). \tag{24}$$

The time evolution of this state is unitary, so $\rho_{AB}(t)$ has the same value as Eq. (24) for the entropy. However, projection always increases the entropy [38,55], so it is easy to show,

$$S[\rho_A(t)\otimes\rho_B(t)] \geqslant S[\rho_{AB}(t)], \tag{25}$$

with $\rho_A(t) = \mathrm{Tr}_B\,[\rho_{AB}(t)]$, etc. Combining Eqs. (24) and (25),

$$\Delta S_A + \Delta S_B \geqslant 0. \tag{26}$$

This is quite general, and applies to any measurement time, starting state, and Hamiltonian $\hat{H}_{AB}$. Again, for a cyclic process A must return to its starting point, so $\oint \Delta S_A = 0$, and $\oint Q \leqslant 0$.

Although the form above is useful in most cases, a stronger form of Eq. (25) can be shown when the projected joint state is

$$\rho_{AB}(t)' = \sum_m \langle m|\rho_{AB}(t)|m\rangle \otimes |m\rangle\langle m|. \tag{27}$$

In this case, since $\mathrm{Tr}[\rho_{AB}(t)'\ln\rho_{AB}(t)'] = \mathrm{Tr}[\rho_{AB}(t)\ln\rho_{AB}(t)']$, the Klein inequality applies to show that

$$S[\rho_{AB}(t)'] \geqslant S[\rho_{AB}(t)]. \tag{28}$$

It should be stressed that the results of this section hold regardless of the lengths of the measurement intervals $\{t_{j+1} - t_j\}$ or driving protocols $[\{\rho_B(t_j), \hat{H}_{AB,j}\}]$. The choice of thermal driving and a Poisson measurement process is not justified in every case. This is especially true for the physical micromaser, where the input state can be precisely controlled and measurement times are usually Gaussian, based on the cavity transit time for each atom.

V. RESULTS

We illustrate the results of the previous sections by comparing the dynamics of the process from Sec. II applied to models of the relaxation dynamics of a single-mode atom-cavity system. In all cases, the system is a single optical mode with Hamiltonian

$$\hat{H}_A = \hbar\omega_A\left(\hat{n}_A + \tfrac{1}{2}\right), \quad \hat{n}_A = a^\dagger a. \tag{29}$$

The cavity begins at time $t = 0$ in its singly excited state ($n_A = 1$). At all times, there is also a two-level atom present, with Hamiltonian

$$\hat{H}_B = \frac{\hbar\omega_B}{2}(|e\rangle\langle e| - |g\rangle\langle g|) = \hbar\omega_B\left(\hat{n}_B - \tfrac{1}{2}\right). \tag{30}$$

According to the process of Sec. II just after every measurement performed on the atom, the atom is reset to a state diagonal in $\hat{H}_B$ with imposed excited- and ground-state probabilities σ_e and σ_g.

A. Jaynes-Cummings model

In the Einstein picture, photons in A can cause excitation of the atom B at a fixed rate. This section uses the model of Sec. II to derive the rate, starting from the transition probabilities of the Jaynes-Cummings model (JCM). It uses an atom-field coupling,

$$\gamma\hat{H}^0_{AB} = \gamma(a^\dagger\sigma_- + a\sigma_+), \tag{31}$$

where

$$\sigma_- \equiv |g\rangle\langle e|, \quad \sigma_+ \equiv |e\rangle\langle g|. \tag{32}$$

The analysis of this model is well known [59–61], and leads to an expression for the transition probabilities $|b_m(t)|^2$ [Eq. (A7)] that depend on the total number of excitations present, $m = \langle\hat{n}_A + \hat{n}_B\rangle$, and which are *periodic* in time. The heat and work exerted by the atom on the cavity are easily found by computing Eqs. (11) and (13) using the model's analytical solution,

$$x(t) \equiv \sum_{n=0}^{\infty} p_n[\sigma_g|b_n(t)|^2 - \sigma_e|b_{n+1}(t)|^2], \tag{33}$$

$$\sigma_e(t) = \sigma_e + x(t), \tag{34}$$

$$\sigma_g(t) = \sigma_g - x(t), \tag{35}$$

$$\langle\Delta H_A(t)\rangle = -\hbar\omega_A x(t), \tag{36}$$

$$\langle\Delta H_B(t)\rangle = \hbar\omega_B x(t). \tag{37}$$

The numbers p_n are the initial occupation probabilities of the cavity, and σ_g (σ_e) is the initial probability of the atom's ground (excited) state. To interpret this correctly, note that both A and B started in uncoupled diagonal states at $t = 0$ and that a measurement on B alone was performed at time t.

All of the quantities in Eqs. (33)–(37) are measurable in this particular model because the JCM is a very special case where unitary evolution only mixes the states $|n-1,e\rangle$ and $|n,g\rangle$. Thus the only allowed transitions are between these two states, and all the results can be neatly expressed in terms of $x(t)$, the average number of photons absorbed by the atom.

To complete the analysis of this model, we apply the assumption of Poisson measurement events (with rate λ) to determine the expected number of absorptions over all measurements. This average is

$$\mathbb{E}[|b_m(t)|^2] = \frac{1}{2}\left(1 - \frac{\lambda^2 + \Delta_c^2}{\lambda^2 + \Delta_c^2 + 4m\gamma^2/\hbar^2}\right), \tag{38}$$

where $\Delta_c = \omega_B - \omega_A$ is the difference between atom and cavity frequencies and $\mathbb{E}[f(t)] \equiv \lambda\int_0^\infty dt\ \exp(-\lambda t)f(t)$. We simplify the result by noting that both fast and slow measurement-rate limits of this equation give identical first-order terms,

$$\lim_{\lambda\to\infty}\mathbb{E}[|b_m(t)|^2] = \lim_{\gamma/\hbar\to 0}\mathbb{E}[|b_m(t)|^2] = \frac{2m\gamma^2/\hbar^2}{\lambda^2 + \Delta_c^2}. \tag{39}$$

Since measurements happen with rate λ, the effective total rate of atomic absorptions in these limits is

$$\lambda\mathbb{E}[x(t)] = \frac{2\lambda\gamma^2/\hbar^2}{\lambda^2 + \Delta_c^2}[\sigma_g\langle\hat{n}_A(0)\rangle - \sigma_e\langle\hat{n}_A(0) + 1\rangle]; \tag{40}$$

the two parts of Eq. (40) show Einstein's simple picture of photon emission and absorption processes occurring with

equal rates [2],

$$dW_{\rm abs}/\Delta E_{\rm abs} = \sigma_g B_g^e \langle \hat{n}_A \rangle dt, \tag{41}$$

$$dW_{\rm em}/\Delta E_{\rm em} = \sigma_e \left(A_e^g + B_e^g \langle \hat{n}_A \rangle \right) dt. \tag{42}$$

All the A, B coefficients are equal to the prefactor of Eq. (40) here because $x(t)$ counts only a single cavity mode at frequency ω_A. In a blackbody, the A coefficient goes as $\omega^2 d\omega$ because more modes contribute [54].

The denominator $\lambda^2 + \Delta_c^2$ is exactly the one that appears in the traditional expression for a Lorentzian line shape. Here, however, the measurement rate λ appears rather than the inverse lifetime of the atomic excited state. The line broadens as the measurement rate increases, and the atom is able to absorb or emit photons further away from its excitation frequency. Only the resonant photons will cause equilibration, while others will cause noise. In the Van Hove limit, $\gamma, \lambda \to 0$ so that the contribution of the resonant photons will dominate. From the importance of Δ_c in this example, we see already that the work of measurement, $\Delta \hat{H}_A + \Delta \hat{H}_B$, will be critical for understanding energy balance.

B. Rabi model

The Rabi model uses the more complete [62] coupling between the field and a dipole oriented in the x direction,

$$\gamma \hat{H}_{AB} = \gamma (a^\dagger + a)(\sigma_+ + \sigma_-). \tag{43}$$

To compute the work and heat under this coupling, we must resort to numerical simulation [64]. Because the process in Fig. 1 is repeated after each measurement, the simulation is carried out by averaging over the distribution of $N = 0, 1, \ldots$ measurement times,

$$P\left(\{t\}_1^N, N \middle| t_j > t_{j-1}\right) = \prod_{j=1}^{N} \lambda^{-1} e^{-\lambda(t_j - t_{j-1})}, \tag{44}$$

starting from the initial state at time $t_0 = 0$. Numerically, the averages plotted are Monte Carlo averages over 5000 samples from Eq. (44). The evolution of the density matrix according to Sec. II is completely determined when the number and times of measurement are known. Average heat and work values [Eqs. (11) and (13)] were computed numerically at each fixed time t_f by taking a weighted average over these Monte Carlo samples of the Poisson process. The sample weights, $\lambda^{-1} e^{-\lambda(t_f - t_j)}$ (where t_j is the last measurement time before t_f) were used to account for the probability that the plotted time t_f is a measurement time.

Figure 3(a) shows the average work and heat computed for the parameters $\omega_A = \omega_B = 2\pi$, $\gamma/\hbar = 0.05$, $\lambda = 10^{-2}$. The quantities shown are cumulative from the starting time, so that $\texttt{sum} - \Delta H_A/\hbar\omega_A = 1/2 - H_A(t)/\hbar\omega_A$. Rabi oscillations can be seen clearly as the photon exchanges with the reservoir (atom). Initially, this increases the entropy of the incoming atom's energy distribution. When there is a strong probability of emission, however, the integrated heat release, $-\int_0^t Q(t')dt'$, shows that the system actually decreases the entropy of the reservoir. This happens because the the reservoir atom is left in a consistent, high-energy, low-entropy state. In this way, the reservoir can extract useful work from the cavity, even during a thermalization process. Figure 3(c) plots the von Neumann entropy of the A system and $S_{\rm tot}$ [the sum of $S_A(t)$ and the integrated heat release], to show that no laws of thermodynamics are broken. Average work was extracted because the system starts in a pure state, but ends in a mixed, equilibrium state. The information entropy of the system itself increases appreciably during the first Rabi cycle. Eventually, the equilibration process ends with the initial excitation energy being transformed into both heat and work. Despite the appearance of Fig. 3(a), the final total emitted heat was generally nonzero for other coupling strengths (not shown).

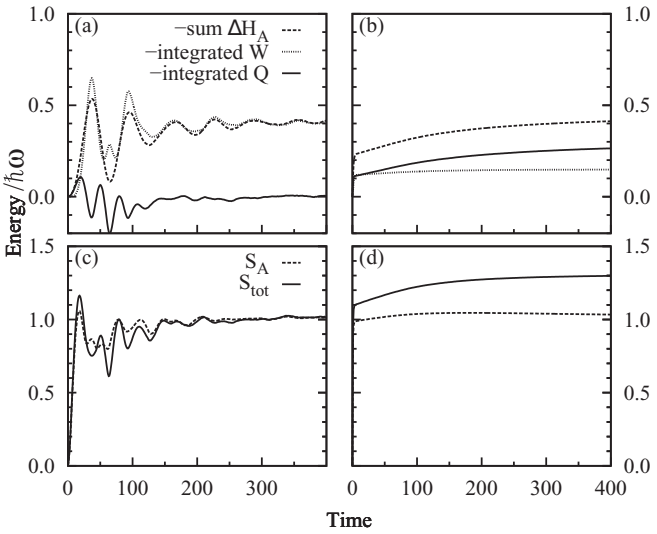

FIG. 3. Work and heat production during decay of a photon in a cavity ($n_A = 1$) coupled to a two-level reservoir via (43), with $\omega_A = \omega_B = 2\pi$, $\gamma = 0.05$, $\lambda = 10^{-2}$, $\beta = 1$. Panels (a) and (b) compare the system energy loss ΔH_A to the work and heat computed from the measured reservoir states [Eqs. (13) and (11)]. Panels (c) and (d) show the information entropy of the A system and the combined entropy change, $S_{\rm tot}(t) = S_A(t) - \int_0^t Q/T > 0$. Note that the traditional calculation of heat [Eq. (2)] gives only $Q \approx \Delta H_A$, $W \approx 0$. Panels (a) and (c) show results for the time evolution of the density matrix using the exact process, while panels (b) and (d) are computed using the weak-coupling approximation of Sec. V C.

C. Comparison to weak coupling

The work and heat defined by Sec. III differ substantially from the standard literature definition based on weak coupling [Eq. (2)]. This is because the earlier definition is based only on the "A" system, without considering the reservoir, "B." It therefore provides no way to use the energy of the atom after interaction for useful work. Equation (2) therefore finds zero work for the process studied here, and classifies ΔH_A entirely as heat lost to the environment.

A better comparison to Eq. (2) is made if we modify the standard weak-coupling scheme to track changes to the reservoir during interaction. Appendix B derives expressions for the time dependence of the joint density matrix ρ_{AB} in the weak-coupling limit and averages over Poisson-distributed

measurement times to find the Lindblad equation,

$$\frac{d\rho_{AB}(t)}{\lambda dt} = -\frac{i\gamma}{\hbar}[\tilde{H}_{AB}(\lambda),\rho_{AB}(0)] + \frac{\gamma^2}{\hbar^2}L'[\rho_{AB}(0)], \quad (45)$$

where

$$\hat{H}_{AB} \equiv \sum_{\omega} \hat{V}_{\omega}, \quad (46)$$

$$\tilde{H}_{AB}(\lambda) = \sum_{\omega} \frac{1}{\lambda - i\omega}\hat{V}_{\omega}, \quad (47)$$

$$L'[\rho] = \sum_{\omega,\omega'} s_{\omega,\omega'}\left(\hat{V}_{\omega}\rho\hat{V}^{\dagger}_{\omega'} - \frac{1}{2}\{\hat{V}^{\dagger}_{\omega'}\hat{V}_{\omega},\rho\}\right) + \frac{i a_{\omega,\omega'}}{2}[\hat{V}^{\dagger}_{\omega'}\hat{V}_{\omega},\rho], \quad (48)$$

$$s_{\omega,\omega'} = \frac{2\lambda - i(\omega-\omega')}{d_{\omega,\omega'}}, \quad (49)$$

$$a_{\omega,\omega'} = \frac{\omega+\omega'}{d_{\omega,\omega'}}, \quad (50)$$

$$d_{\omega,\omega'} = (\lambda - i\omega)(\lambda + i\omega')[\lambda - i(\omega-\omega')]. \quad (51)$$

This equation reduces to the traditional dynamics [16] in the Van Hove limit ($\gamma,\lambda \to 0$ with $\gamma^2/\lambda \to$ const). Note that the sums run over both positive and negative transition frequencies ω and that these quantities have the symmetries $\hat{V}^{\dagger}_{\omega} = \hat{V}_{-\omega}$, $s^*_{\omega,\omega'} = s_{\omega',\omega}$, $d^*_{\omega,\omega'} = d_{\omega',\omega}$, and $a^*_{\omega,\omega'} = a_{\omega',\omega}$. The canonical Lindblad form can be obtained by diagonalizing the matrix $[s_{\omega,\omega'}]$. Numerical simulations of the Lindblad equation were carried out using QuTiP [64].

To make the comparison with weak coupling, we carried out the same sampling over Poisson-distributed measurement times as in the last section, but replaced the propagator with the integrated form of Eq. (45). As before, the heat and work were computed from the joint density matrix at the beginning and end of each measurement interval.

Figures 3(b) and 3(d) show that the initial $\cos^2$ shape and Rabi oscillation structure are lost in the weak-coupling limit. Instead, the L' propagator creates a fast initial loss of cavity energy followed by exponential decay toward the steady state. Nevertheless, the observed decay rate and eventual steady states match very well between the two methods. The total evolved heat shows a discrepancy between methods because the fast initial loss in the L' propagator quickly mixes ρ_B.

The only source of differences between exact evolution and the Lindblad form of Eq. (45) is the additional dissipation brought about by smearing over the measurement times. Because a dissipative propagator (L') is used within a measurement interval, some quantum correlations with the reservoir are not captured. Neglecting these correlations leads to artificial heat release. This effect may be exaggerated here because the two systems are at a resonance condition.

Figure 4 illustrates the effect of using the weak-coupling propagator (L') at different measurement rates. Without the trace over the environment—i.e., at a slow measurement rate as in panel (a)—L' just gives the approximation to $\rho_{AB}(t)$ from second-order perturbation theory. This actually decays *faster* than when repeated projection is used—i.e., at a fast measurement rate as in panel (d)—because the environment loses its memory after each projection [55]. Both the fast initial relaxation and slow exponential tail (due to measurement) are visible in the figure.

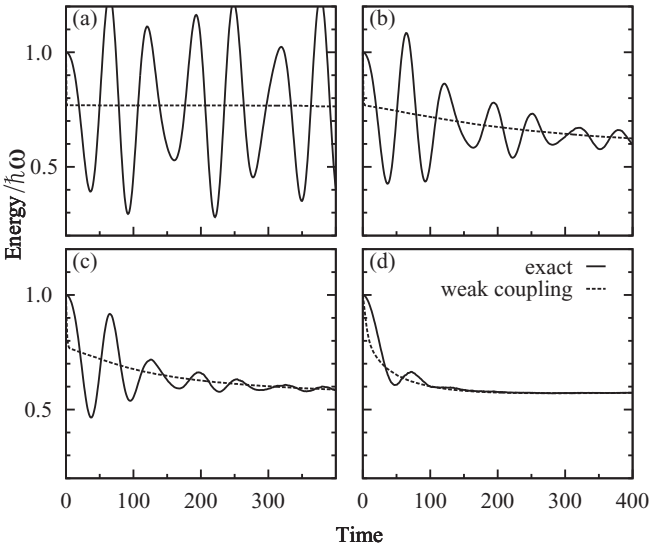

FIG. 4. Decay of the system simulated in Fig. 3 from an excited state [$E_A(0) = \hbar\omega_A$] at different values of the measurement rate. Panels (a)–(d) have rates $\lambda = 10^{-4}$, 5×10^{-3}, 10^{-2}, and 5×10^{-2}, respectively. The exact propagator is compared with the weak-coupling propagator under the same repeated measurement process. The shape of the decay to steady-state behavior is a combination of fast energy exchange due to Rabi oscillations and the slower process of memory loss through repeated measurement.

This crossover highlights a tradeoff in choosing the time scale for simulations employing weak-coupling approximations. Although a slow measurement rate λ is needed to minimize the effect of measurement back reaction on the system energy, agreement with the exact dynamics is better at fast measurement rates. Actually performing repeated measurements has important energetic and dynamical consequences for the system.

VI. MINIMUM ACHIEVABLE TEMPERATURE

Simulation results of the last section reveal that even as the reservoir temperature approaches zero, the probability of the first excited state does not vanish. In fact, the results very nearly resemble a Gibbs distribution at elevated temperatures. As the reservoir goes to absolute zero, the effective system temperature levels off to a constant, minimum value.

This section gives both intuitive and rigorous arguments showing that this is a general phenomenon originating from work added during the measurement process. First, observe that the total Hamiltonian $\hat{H}$ is preserved during coupled time evolution. When allowed by the transitions in $\hat{H}_{AB}$ (i.e., when $[\hat{H},\hat{H}_{AB}] \neq 0$), a portion of that total energy will oscillate between $\hat{H}_A + \hat{H}_B$ and $\hat{H}_{AB}$. Consider, for example, a dipole-dipole interaction, $\hat{H} = \hat{x}_A^2 + \hat{p}_A^2 + \hat{x}_B^2 + \hat{p}_B^2 + \gamma\hat{x}_A\hat{x}_B$. At equilibrium, the individual systems have $\langle\hat{x}\rangle = 0$, but the coupled system polarizes so that $\langle\hat{H}_{AB}\rangle < 0$.

Intuitively, the joint system can be pictured as relaxing to a thermal equilibrium at an elevated temperature $1/\beta'$. The initial density matrix at each restart, $\rho_A(\beta') \otimes \rho_B(\beta)$, would

then look like an instantaneous fluctuation of

$$\rho_{AB}(\beta') = e^{-\beta'\hat{H}}/Z_{AB}(\beta'), \tag{52}$$

where $\langle \hat{H}_{AB}\rangle = 0$ is too high and $\langle \hat{H}_B\rangle$ is too low.

At steady state, $\langle \hat{H}_A\rangle$ must be the same at the beginning and end of every measurement cycle. This allows the equilibrium argument above to determine β' by self-consistency,

$$\langle \mathbb{E}[\hat{H}_B(t)] - \hat{H}_B(\beta)\rangle = -\gamma\langle \mathbb{E}[\hat{H}_{AB}(t)]\rangle. \tag{53}$$

If equilibrium at $\beta' = 1/k_B T'$ is reached by the average measurement time, then expanding $\langle \hat{H}_B(\beta') - \hat{H}_B(\beta)\rangle$ yields

$$\Delta T \simeq \frac{-\gamma\langle \mathbb{E}[\hat{H}_{AB}(t)]\rangle}{C_{V,B}}, \tag{54}$$

where $C_{V,B}$ is the heat capacity of the reservoir system.

It is well known that quantum mechanical degrees of freedom freeze out at temperatures that are fractions of their first excitation energy (ΔE_1). Since the heat capacity when $\beta^{-1} < \Delta E_1$ goes to zero, while the interaction energy should remain nonzero, this intuitive argument suggests that the temperature of the system cannot go much below $\Delta E_1/k_B$.

To be more quantitative, $\langle \mathbb{E}[\hat{H}_{AB}(t)]\rangle$ can be estimated in the weak-coupling limit from the second-order perturbation theory of Appendix B. This comparison considers the case $\Delta_c = 0$, since the stationary state where $\Delta_c \neq 0$ is known to be noncanonical. Also, the JCM with rotating wave approximation is too idealistic, since when $\Delta_c = 0$ no off-resonance interactions can occur—so $\hat{H}_{AB}$ commutes with $\hat{H}$ and the minimum temperature argument does not apply. In other words, in the rotating wave approximation, the number of absorption events $x(t)$ always increases the energy of the atom and decreases the energy of the cavity by the same amount.

However, if the more physical interaction Hamiltonian [Eq. (43)] is used, then the weak-coupling theory should also include transitions between $0,g$ and $1,e$. The average number of simultaneous excitations must be tracked separately, since it increases both the energy of the atom and cavity. Using Eq. (48) with $\omega_A = \omega_B = \omega$, this average is

$$\langle a^\dagger\sigma_+ + a\sigma_-\rangle = \frac{2\gamma^2/\hbar^2}{\lambda^2 + (2\omega)^2}(\sigma_g\langle \hat{n}_A + 1\rangle - \sigma_e\langle \hat{n}_A\rangle). \tag{55}$$

In the low-temperature limit, only the probabilities of the four lowest-lying states, labeled $p_{0/1}\sigma_{g/e}$, contribute substantially. Inserting Eq. (55) into the weak-coupling dynamics [Eq. (45)],

$$\frac{\partial\langle \hat{H}_A\rangle}{\partial t} = \frac{2\frac{\omega}{\lambda}\gamma^2/\hbar}{\left(\frac{\lambda}{2\omega}\right)^2 + 1}\left[\left(\tfrac{\lambda}{2\omega}\right)^2(p_0 - p_1) + \sigma_e p_0 - \sigma_g p_1\right]. \tag{56}$$

This result applies whenever $\hat{H}_{AB}$ allows for both $0,e \leftrightarrow 1,g$ and $0,g \leftrightarrow 1,e$ transitions with with equal weight and respective energy differences of zero and $2\hbar\omega$. Equation (56) can be solved for steady state to find

$$\frac{p_1}{p_0} = \frac{\left(\frac{\lambda}{2\omega}\right)^2 + \sigma_e}{\left(\frac{\lambda}{2\omega}\right)^2 + \sigma_g}. \tag{57}$$

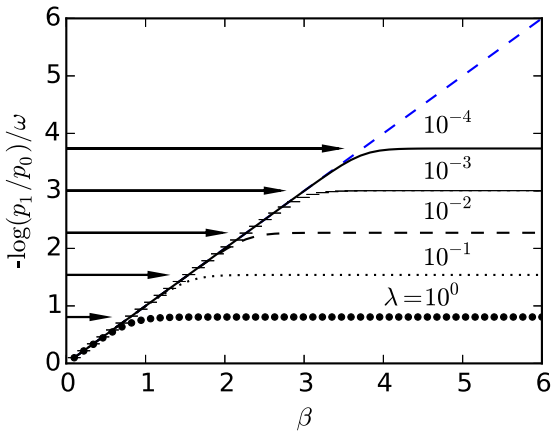

FIG. 5. Steady-state inverse temperature vs reservoir β. The arrows plot the limiting value of $-\omega^{-1}\ln p_1/p_0$ from Eq. (58). Each line represents the steady states found using a fixed measurement rate λ as the reservoir temperature varies. Their y values were computed from the steady-state probabilities for simulation in the weak-coupling limit [Eq. (B11)].

In the low-temperature limit,

$$\lim_{\sigma_g\to 1}\frac{p_1}{p_0} = \frac{\left(\frac{\lambda}{2\omega}\right)^2}{\left(\frac{\lambda}{2\omega}\right)^2 + 1}. \tag{58}$$

This argument brings the energy-time uncertainty principle into sharp focus. If the measurement rate is on the order of the transition frequency ω then p_1/p_0 can be of order 1, making absolute zero unreachable regardless of the coupling strength γ or the reservoir temperature determining σ_e/σ_g. On the other hand, as the relative measurement rate λ/ω approaches zero the thermodynamic equilibrium condition $\sigma_e p_0 = \sigma_g p_1$ dominates. In the limit where measurements are performed very slowly, transitions that do not conserve the energy of the isolated systems are effectively eliminated.

Figure 5 illustrates these conclusions by solving numerically for the steady states of the Rabi model (Sec. V B) as a function of environmental temperature, $k_B T = \beta^{-1}$. The limiting predictions of Eq. (58) are drawn as arrows for each simulated value of the measurement rate λ. For high reservoir temperatures and low measurement rates, the system's steady-state probabilities follow the canonical distribution with the same temperature as the reservoir (since they fall on a straight line). When the reservoir temperature is lowered below a limiting value, the system is unable to respond—effectively reaching a minimum temperature determined by Eq. (58). Effects from the minimum temperature can be controlled by lowering the measurement rate.

VII. CONCLUSIONS

A measurement process is required in order to avoid the EPR paradox for defining heat and work in a quantum setting. However, continually measuring the energy of an interacting quantum system has important energetic and dynamical consequences for the system. Traditional definitions of work and heat avoid this problem because they assume infinitely slow measurement rates. Our process shows that quantum

systems under repeated measurement do not always reach canonical (Boltzmann-Gibbs) steady states. Instead, the steady state of a quantum system depends both on its coupling to an external environment and the rate of measurement.

This analysis creates a less restrictive proof of the unattainability of absolute zero, which is one part of the third law of thermodynamics [65,66]. Other proofs in the literature have arrived at similar conclusions for the minimum achievable temperature by examining specific models for the optimal rate of cooling in quantum engines under weak coupling [67], or in heat exchangers using scattering theory [68]. A general minimum temperature argument was constructed in Ref. [69] by maximizing the probability that the system is set to the ground state over arbitrary unitary coupling to a reservoir. The present result (Sec. VI) applies generally to all systems and reservoirs that follow the dynamic measurement process considered in this work.

The presence of a measurement rate in the theory indicates the importance of the outside observer—a familiar concept in quantum information [5]. Most experiments on quantum information have been analyzed in the context of a Lindblad master equation, whose standard interpretation relies on associating a measurement rate to every dissipative term. All energy changes arising from these terms were previously assumed to be lost as heat. We have shown that every process with a measurement rate can be used as a source and sink for work as well as heat. This use creates an alternative to time-dependent coupling Hamiltonians required by other theories.

Our argument was based on accounting for heat and work during each single measurement step. We showed that averaging over Poisson-distributed measurement times rederives the master equation as the approximation to this process in the limit of weak coupling. The result agrees with standard line-shape theory and extends thermodynamics to fast, strongly coupled measurement processes.

The physical consequences of the measurement rate will become increasingly important as quantum experiments push for greater control [51]. However, they also present an opportunity to probe the measurement rule and energy-time uncertainty principle. For the micromaser, the rate *seems* to be the number of atoms sent through the cavity per unit time—since every atom that leaves the cavity is measured via its interaction with the outside environment. It is not, however, because even there the atoms can be left isolated and held in a superposition state indefinitely, leading to entanglement between successive particles [61]. Most generally, the number of measurements per unit time is determined by the rate at which information can leak into the environment. If information leaks quickly, the amount of energy exchanged can be large and the minimum effective temperature of the system will be raised. If information leaks slowly, the work done by measurement will be nearly zero, and the quantum system will more closely approach the canonical distribution. By the connection to the width of spectroscopic lines, this rate is closely related to the excited-state lifetime.

This model presents an experimentally motivated and thermodynamically consistent treatment of heat and work exchange in the quantum setting. By doing so, it also raises questions about the thermodynamics of measurement. First, the explicit connection to free energy and entropy of reservoir states provides an additional source of potential work that may be extracted from coupling. Connecting multiple systems together or adding further dynamic details to the measurement process (rather than simple projection) are well posed within this framework. Second, we have shown the conditions needed for the present definitions to reduce to well-known expressions in the literature. Third, although the initial process was defined in terms of wave functions, the average heat and work is defined in terms of the density matrices. Definitions [Eqs. (11) and (13)] still apply when the density matrix consists of a single state, but the repeated measurement projecting to a single wave function has a subtly different interpretation. The difference (not investigated here) is related to Landauer's principle [22,35], since measuring the exact state from the distribution, $\rho_A \otimes \rho_B$, carries a separate "recording" cost.

There have been many other investigations on thermodynamics of driven, open quantum systems. The restriction to time-independent Hamiltonians in this work differs from most others, which assume a prespecified, time-dependent $\hat{H}_A(t)$. To make a comparison, either the cycle should be modified as described in Sec. III A or work at each time step in such models must be redefined to count only energy that is stored in a time-independent Hamiltonian for the central system H_A.

Quantum jump and power measurement based methods assume, following weak-coupling definitions, that heat is defined as all energy exchange with a "dissipative" reservoir. There, work is supplied by the time dependence of the Hamiltonian. An interesting point of the present study is that heat may be more closely identified with changes to the von Neumann entropy of the B system, and by strong subadditivity, to the time-dependent entropy of A. The energy exchange with the reservoir is only indirectly connected to the heat exchange through Eq. (20). The fact that this becomes exact in the Van Hove limit explains the role of the steady state for A and observations by many authors that the work of measurement is the source of nonapplicability of fluctuation theorems [10–12,26,31].

When $[\hat{H}, \hat{H}_{AB}] = 0$, then energy is conserved between the subsystems ($\Delta H_A + \Delta H_B = 0$). In this case, the measurement back action disappears, and the fluctuation theorem for ΔH_A is given by the formalism of Ref. [13]. It should also be possible to derive a forward fluctuation theorem (not restricted to time reversal) for predicting the force- flux relationships along the lines of Ref. [15].

The process studied here retains a clear connection to the experimental measurement process, and is flexible enough to compute heat and work for continuous feedback control. In view of the near identity between our Eq. (58) and Eq. (10) of Ref. [27] [also similar in form to Eq. (77) of Ref. [69] it is very likely that recent experimental deviations from the fluctuation theorem are due to the phenomenon of minimum temperature, as well as to differences between traditional, system-centric, and the present, observational, definitions of heat and work.

ACKNOWLEDGMENTS

I thank S. Deffner, B. Space, and B. Gardas for helpful discussions. This work was supported by the University of

South Florida Research Foundation and NSF MRI CHE-1531590.

APPENDIX A: ANALYSIS OF THE MICROMASER

Exact numerical results are known for the micromaser in the rotating wave approximation—a single-qbit system (B) in state e or g coupled to a single mode of an optical cavity (A) in a Fock state, $n = 0,1,\ldots$ [59–61]. The Hamiltonian is known as the Jaynes-Cummings model (JCM) and is given by Eq. (31). The rotating wave approximation neglects a term,

$$\gamma \hat{H}'_{AB} = \gamma(a_A^\dagger a_B^\dagger + a_A a_B), \tag{A1}$$

in the Hamiltonian causing simultaneous excitation of the qbit and cavity that is present in the Rabi model [Eq. (43)]. It is usually justified when the two frequencies, ω_A and ω_B, are near resonance [70], but is critical for reproducing some quantum effects [9].

The JCM is an idealized model for understanding experiments on the one-photon micromaser. There, a sequence of atoms are passed through an optical cavity tuned to a resonant frequency ω_A. The work exchange between the field and a passing atom is realized when the energy of the exiting atom is measured. This will project the environment into a state with known excitation, $n_B = 1$ or 0.

For completeness, we derive the solution of the JCM given in Eq. (33). The solution is well known [7,59,60], but is restated here because the notation is slightly different. For states with $m > 0$ total excitations, the time-evolution operator decomposes into a 2×2 block diagonal [70],

$$\begin{bmatrix} \langle n-1,e|\psi(t)\rangle \\ \langle n,g|\psi(t)\rangle \end{bmatrix} = e^{-i\omega_A t(n-1/2)} \times \begin{bmatrix} a_n(t) & b_n(t) \\ b_n(t) & a_n(t)^* \end{bmatrix} \begin{bmatrix} \langle n-1,e|\psi(0)\rangle \\ \langle n,g|\psi(0)\rangle \end{bmatrix}, \tag{A2}$$

with the definitions [59]

$$\Omega_n = \frac{2\gamma}{\hbar}\sqrt{n}, \tag{A3}$$

$$\Delta_c = \omega_B - \omega_A, \tag{A4}$$

$$\Omega_n'^2 = \Omega_n^2 + \Delta_c^2, \tag{A5}$$

$$a_n(t) = \cos(\Omega'_n t/2) - \frac{i\Delta_c}{\Omega'_n}\sin(\Omega'_n t/2), \tag{A6}$$

$$b_n(t) = -\frac{i\Omega_n}{\Omega'_n}\sin(\Omega'_n t/2). \tag{A7}$$

Starting at $t = 0$ from $|n-1\rangle\langle n-1| \otimes |e\rangle\langle e|$ gives

$$\rho_{AB}(t) = \begin{bmatrix} |n-1,e\rangle \\ |n,g\rangle \end{bmatrix}^T \begin{bmatrix} |a_n(t)|^2 & -a_n(t)b_n(t) \\ a_n^*(t)b_n(t) & |b_n(t)|^2 \end{bmatrix} \times \begin{bmatrix} \langle n-1,e| \\ \langle n,g| \end{bmatrix}. \tag{A8}$$

Starting, instead, at $t = 0$ from $|n\rangle\langle n| \otimes |g\rangle\langle g|$ gives

$$\rho_{AB}(t) = \begin{bmatrix} |n-1,e\rangle \\ |n,g\rangle \end{bmatrix}^T \begin{bmatrix} |b_n(t)|^2 & a_n(t)b_n(t) \\ -a_n^*(t)b_n(t) & |a_n(t)|^2 \end{bmatrix} \times \begin{bmatrix} \langle n-1,e| \\ \langle n,g| \end{bmatrix}. \tag{A9}$$

Because of the simplicity of this system, measuring the atom also projects the cavity into a Fock state. This simplifies the analysis, since we only need to track the pure probabilities p_n. Assuming the incoming atomic states are chosen to be pure e or g at random (with probabilities σ_e or σ_g, respectively),

$$p_n(t) = p_n(0) + |b_{n+1}(t)|^2(\sigma_g p_{n+1} - \sigma_e p_n) - |b_n(t)|^2(\sigma_g p_n - \sigma_e p_{n-1}). \tag{A10}$$

Equation (A10) uses the fact that $b_0 = 0$. This expression for the density matrix immediately after measurement can be used to make exact calculations of the work and heat in the JCM.

This master equation has a nontrivial steady state at $p_n = p_0(\frac{\sigma_e}{\sigma_g})^n$. The existence of this steady state, and the fact that the cavity does not have a canonical distribution, even when the atom does ($\sigma_e/\sigma_g = e^{-\beta\hbar\omega_B}$), were noted by Jaynes [70]. Experimentally, relaxation to the canonical distribution occurs because of imperfect isolation of the cavity, which allows thermalization interactions with external resonant photons and results in a near-canonical (but not perfect) steady state [60]. Such interactions could easily be added to the present model, but for clarity this analysis focuses on interaction with the single reservoir system B.

Equation (38) is derived by averaging over the distribution of measurement times,

$$\mathbb{E}[|b_n(t)|^2] = \int_0^\infty \lambda e^{-\lambda t} dt\ \frac{\Omega_n^2}{\Omega_n'^2}\sin^2(\Omega'_n t/2). \tag{A11}$$

In the limit of many measurements ($T/t \to \infty$), this expectation gives the rate of transitions (and from those the rates of heat and work) per average measurement interval. Note that for the physical micromaser setup, the interaction time is set by the velocity of the atom and the cavity size—resulting in a narrow Gaussian distribution rather than the Poisson process studied here.

APPENDIX B: WEAK-COUPLING LIMIT

The classical Van Hove limit was investigated in detail by Spohn and Lebowitz [16], who showed generally that thermal equilibrium is reached by ρ_A in this limit irrespective of the type of coupling interaction $\hat{H}_{AB}$. First, the interaction strength γ must tend to zero so that only the leading-order term in the interaction remains. This makes the dynamics of $\rho_A(t) = \mathrm{Tr}_B[\rho_{AB}(t)]$ expressible in terms of two-point time-correlation functions for the reservoir. We use the term "weak-coupling limit" in the text to refer only to $\gamma \to 0$.

We use the term "Van Hove limit" to refer to taking the weak coupling first, followed by assuming an infinitely slow measurement process. We derive the long-time limit below as $\lambda \to 0$. This enforces energy conservation because time evolution causes off-diagonal matrix elements to oscillate and average to zero over long enough time scales.

Finally, the Gibbs ensemble is found to be stationary by combining energy conservation with the detailed balance condition obeyed by the reservoir,

$$\mathrm{Tr}_B[e^{-\beta\hat{H}_B}\hat{A}(0)\hat{B}(t)] = \mathrm{Tr}[e^{-\beta\hat{H}_B}\hat{B}(t-i\beta)\hat{A}(0)], \quad \text{(B1)}$$

which enforces for the A system,

$$e^{-\beta E_n^A}B_n^m = e^{-\beta E_m^A}B_m^n. \quad \text{(B2)}$$

The time dependence of the operators in this equation is defined by the Heisenberg picture, below.

Because Sec. V C requires expressions for the time dependence of both ρ_A and ρ_B, this section rederives the weak-coupling limit without taking the partial trace. The time dependence of ρ can be found from second-order perturbation theory,

$$\theta_{AB}(t) = \rho_{AB}(0) - \frac{i\gamma}{\hbar}\int_0^t dx\ [\hat{H}_{AB}(x),\rho_{AB}(0)] + O\left(\tfrac{\gamma^3}{\hbar^3}\right) - \frac{\gamma^2}{\hbar^2}\int_0^t ds\int_0^s dx\ [\hat{H}_{AB}(s),[\hat{H}_{AB}(x),\rho_{AB}(0)]], \quad \text{(B3)}$$

where $\rho_{AB}(0) = \rho_A \otimes \rho_B(0)$. This equation uses the following notation for the density matrix and time dependence in the interaction representation:

$$\theta_{AB}(t) = U_0^{-t}\rho_{AB}(t)U_0^t, \quad \text{(B4)}$$

$$\hat{H}_{AB}(t) = U_0^{-t}\hat{H}_{AB}U_0^t \quad \text{(B5)}$$

with time-evolution operator

$$U_0 = e^{-i(\hat{H}_A+\hat{H}_B)/\hbar}. \quad \text{(B6)}$$

The time evolution can be written more explicitly by decomposing $\hat{H}_{AB}$ into transitions between joint system-reservoir states (m to k) with energy difference $\omega_k - \omega_m$,

$$\hat{H}_{AB}(t) = \sum_\omega \hat{V}_\omega e^{i\omega t} \quad \text{(B7)}$$

where

$$\hat{V}_\omega \equiv \sum_{k,m\,:\,\omega_k-\omega_m=\omega} |k\rangle\langle k|\hat{H}_{AB}|m\rangle\langle m|. \quad \text{(B8)}$$

Equation (45) in the text is derived by averaging each term in Eq. (B3) over a Poisson distribution for the measurement time t,

$$\mathbb{E}[\theta(t)] = \lambda\int_0^\infty dt\ e^{-\lambda t}\theta(t) \quad \text{(B9)}$$

$$= \rho_{AB}(0) - \frac{i\gamma}{\hbar}[\tilde{H}_{AB}(\lambda),\rho_{AB}(0)] + \frac{\gamma^2}{\hbar^2}L'[\rho_{AB}(0)]. \quad \text{(B10)}$$

When $\lambda \to 0$, transitions where energy is conserved between the A and B systems ($\omega = 0$) dominate in the sum, resulting in a net prefactor of $(\gamma/\lambda\hbar)^2$. The transition rate is then $\gamma^2/\hbar^2\lambda$—exactly the combination that is kept constant in the Van Hove limit. In this limit, tracing over B in Eq. (48) should recover Eq. (III.19) of Ref. [16].

By applying the interaction part of Eq. (48) to the time evolution with rate λ, the effective master equation in the weak-coupling limit becomes

$$\frac{\partial\rho_A}{\partial t} = -\frac{i}{\hbar}[\hat{H}_A,\rho_A(t)] + \frac{\gamma^2\lambda}{\hbar^2}\mathrm{Tr}_B[L'[\rho_A(t)\otimes\rho_B(0)]]. \quad \text{(B11)}$$

For the JCM, there is just one $\hat{V}_{\Delta_c} = a\sigma_+$. The time evolution in this picture reproduces the exact result, Eq. (40).

APPENDIX C: FAST COUPLING LIMIT

For the atom-field system, it was shown that the transition rate approached the same value in both the weak-coupling and infinitely fast measurement case. To find the general result for the Poisson measurement process as $\lambda \to \infty$, note that the Taylor series expansion of the time average turns into an expansion in powers of λ^{-1},

$$\lambda\int_0^\infty dt\ e^{-\lambda t}\theta(t) = \sum_{k=0}^\infty \lambda^{-k}\theta^{(k)}(t). \quad \text{(C1)}$$

It is elementary to calculate successive derivatives, $\theta^{(k)}$, by plugging into

$$\frac{\partial\theta(t)}{\partial t} = -\frac{i\gamma}{\hbar}[\hat{H}_{AB}(t),\theta(t)]. \quad \text{(C2)}$$

The average measured θ after a short interaction time on the order of λ^{-1} is therefore

$$\mathbb{E}[\theta(t)] = \rho_{AB}(0) - \frac{i\gamma}{\lambda\hbar}[\hat{H}_{AB},\rho_{AB}(0)] + \frac{\gamma}{\lambda^2\hbar^2}[[\hat{H}_A+\hat{H}_B,\hat{H}_{AB}],\rho_{AB}(0)] + \frac{\gamma^2}{\lambda^2\hbar^2}\left(2\hat{H}_{AB}\rho_{AB}(0)\hat{H}_{AB} - \left\{\hat{H}_{AB}^2,\rho_{AB}(0)\right\}\right) + O\left(\frac{\gamma^3}{\lambda^3\hbar^3}\right). \quad \text{(C3)}$$

We can immediately see that this limit is valid when the measurement rate is faster than $\gamma/\hbar$ measurements per second. The $O(\gamma)$ terms are in the form of a time propagation over the average measurement interval λ^{-1}. They have only off-diagonal elements, and do not contribute to $\langle\hat{H}_A\rangle$ or $\langle\hat{H}_B\rangle$.

The third term has the familiar Lindblad form, which immediately proves a number of important consequences. First, all three terms are trace free and totally positive. Next, this term introduces dissipation towards a stationary state for ρ. For a system under infinitely fast repeated measurement, the $O(\gamma)$ terms do not contribute to Tr_B, and the density matrix evolves according to

$$\dot{\rho}_A(t) = -\frac{i}{\hbar}[\hat{H}_A,\rho_A(t)] - \frac{\gamma^2}{\lambda\hbar^2}\mathrm{Tr}_B[[\hat{H}_{AB},[\hat{H}_{AB},\rho_A\otimes\rho_B(0)]]]. \quad \text{(C4)}$$

A more explicit representation is possible by defining the submatrices,

$$[\hat{V}^{nm}]_{ij} = [\hat{H}_{AB}]_{in,jm}. \quad \text{(C5)}$$

These have the symmetry $\hat{V}^{nm} = \hat{V}^{\dagger mn}$, so

$$-[[\hat{H}_{AB},[\hat{H}_{AB},\rho_A \otimes \rho_B(0)]]]_{m,m} = \sum_n p_n^B 2\hat{V}^{mn}\rho_A\hat{V}^{\dagger mn} - p_m^B\{\hat{V}^{mn}\hat{V}^{\dagger mn},\rho_A\}. \quad \text{(C6)}$$

For the JCM, this gives

$$\lambda\langle x\rangle = \frac{2\gamma^2}{\hbar^2\lambda}(\sigma_g\langle n\rangle - \sigma_e\langle n+1\rangle). \quad \text{(C7)}$$

The stationary state of this system will usually not be in the canonical, Boltzmann-Gibbs form. In fact, the prefactor does not depend on the cavity-field energy mismatch Δ_c, so it gives atomic transitions regardless of the wavelength of the light.

This phenomenon is an explicit manifestation of the energy-time uncertainty principle. In the long-time limit of Sec. B, energy-preserving transitions dominated over all possibilities. In the short-time limit of this section, all the transitions contribute equally, and the energy difference caused by a transition could be infinitely large. In between, energy conservation (and convergence to the canonical distribution) depends directly on the smallness of the measurement rate λ.

[1] The first part of this argument is demonstrated for "strong-coupling" Hamiltonians by Eq. (3) and the second part by notes following Eq. (1).

[2] A. Einstein, On the quantum theory of radiation, Phys. Zeit. **18**, 121 (1917); Translation by Alfred Engel, in *The Collected Papers of Albert Einstein* (Princeton University Press, Princeton, NJ, 1997), Vol. 6, p. 220, http://einsteinpapers.press.princeton.edu/vol6-trans/232.

[3] A. Einstein, B. Podolsky, and N. Rosen, Can quantum-mechanical description of physical reality be considered complete?, Phys. Rev. **47**, 777 (1935).

[4] A. Einstein, Physics and reality, J. Franklin Inst. **221**, 349 (1936).

[5] H. M. Wiseman and L. Diósi, Complete parameterization, and invariance, of diffusive quantum trajectories for Markovian open systems, Chem. Phys. **268**, 91 (2001).

[6] R. Chetrite and K. Mallick, Quantum fluctuation relations for the lindblad master equation, J. Stat. Phys. **148**, 480 (2012).

[7] J. M. Horowitz, Quantum-trajectory approach to the stochastic thermodynamics of a forced harmonic oscillator, Phys. Rev. E **85**, 031110 (2012).

[8] F. W. J. Hekking and J. P. Pekola, Quantum Jump Approach for Work and Dissipation in a Two-Level System, Phys. Rev. Lett. **111**, 093602 (2013).

[9] N. Erez, G. Gordon, M. Nest, and G. Kurizki, Thermodynamic control by frequent quantum measurements, Nature (London) **452**, 724 (2008).

[10] B. Prasanna Venkatesh, G. Watanabe, and P. Talkner, Quantum fluctuation theorems and power measurements, New J. Phys. **17**, 075018 (2015).

[11] K. Funo, Yu Watanabe, and M. Ueda, Integral quantum fluctuation theorems under measurement and feedback control, Phys. Rev. E **88**, 052121 (2013).

[12] S. Deffner, J. Pablo Paz, and W. H. Zurek, Quantum work and the thermodynamic cost of quantum measurements, Phys. Rev. E **94**, 010103(R) (2016).

[13] G. Manzano, J. M. Horowitz, and J. M. R. Parrondo, Nonequilibrium potential and fluctuation theorems for quantum maps, Phys. Rev. E **92**, 042127 (2015).

[14] R. Kosloff, Quantum thermodynamics: A dynamical viewpoint, Entropy **15**, 2100 (2013).

[15] D. M. Rogers and S. B. Rempe, Irreversible thermodynamics, J. Phys., Conf. Ser. **402**, 012014 (2012).

[16] H. Spohn and J. L. Lebowitz, Irreversible thermodynamics for quantum systems weakly coupled to thermal reservoirs, Adv. Chem. Phys. **38**, 109 (1978).

[17] R. Alicki, The quantum open system as a model of the heat engine, J. Phys. A: Math. Gen. **12**, L103 (1979).

[18] E. Geva and R. Kosloff, A quantum-mechanical heat engine operating in finite time. a model consisting of spin-1/2 systems as the working fluid, J. Chem. Phys. **96**, 3054 (1992).

[19] T. D. Kieu, The Second Law, Maxwell's Demon, and Work Derivable from Quantum Heat Engines, Phys. Rev. Lett. **93**, 140403 (2004).

[20] H. T. Quan, Y.-x. Liu, C. P. Sun, and F. Nori, Quantum thermodynamic cycles and quantum heat engines, Phys. Rev. E **76**, 031105 (2007).

[21] M. Esposito, R. Kawai, K. Lindenberg, and C. Van den Broeck, Quantum-dot carnot engine at maximum power, Phys. Rev. E **81**, 041106 (2010).

[22] S. W. Kim, T. Sagawa, S. De Liberato, and M. Ueda, Quantum Szilard Engine, Phys. Rev. Lett. **106**, 070401 (2011).

[23] L. Diósi, *A Short Course in Quantum Information Theory*, Lecture Notes in Physics Vol. 827, 2nd ed. (Springer, Heidelberg, 2011).

[24] H. Li, J. Zou, W.-L. Yu, L. Li, B.-M. Xu, and B. Shao, Negentropy as a source of efficiency: A nonequilibrium quantum Otto cycle, Eur. Phys. J. D **67**, 134 (2013).

[25] H. T. Quan, S. Yang, and C. P. Sun, Microscopic work distribution of small systems in quantum isothermal processes and the minimal work principle, Phys. Rev. E **78**, 021116 (2008).

[26] C. Jarzynski and D. K. Wójcik, Classical and Quantum Fluctuation Theorems for Heat Exchange, Phys. Rev. Lett. **92**, 230602 (2004).

[27] Y. Utsumi, D. S. Golubev, M. Marthaler, K. Saito, T. Fujisawa, and G. Schön, Bidirectional single-electron counting and the fluctuation theorem, Phys. Rev. B **81**, 125331 (2010).

[28] B. Küng, C. Rössler, M. Beck, M. Marthaler, D. S. Golubev, Y. Utsumi, T. Ihn, and K. Ensslin, Irreversibility on the Level of Single-Electron Tunneling, Phys. Rev. X **2**, 011001 (2012).

[29] J. V. Koski, T. Sagawa, O.-P. Saira, Y. Yoon, A. Kutvonen, P. Solinas, M. Möttönen, T. Ala-Nissila, and J. P. Pekola, Distribution of entropy production in a single-electron box, Nat. Phys. **9**, 644 (2013).

[30] J. P. Pekola, Towards quantum thermodynamics in electronic circuits, Nat. Phys. **11**, 118 (2015).

[31] C. Jarzynski, H. T. Quan, and S. Rahav, Quantum-Classical Correspondence Principle for Work Distributions, Phys. Rev. X **5**, 031038 (2015).

[32] H. Tasaki, Jarzynski relations for quantum systems and some applications, arXiv:cond-mat/0009244.

[33] P. Talkner and P. Hänggi, The Tasaki-Crooks quantum fluctuation theorem, J. Phys. A **40**, F569 (2007); see note in text.

[34] V. Vedral, The role of relative entropy in quantum information theory, Rev. Mod. Phys. **74**, 197 (2002).

[35] E. Lutz and S. Ciliberto, Information: From Maxwell's demon to Landauer's eraser, Phys. Today **68**(9), 30 (2015).

[36] J. M. R. Parrondo, J. M. Horowitz, and T. Sagawa, Thermodynamics of information, Nat. Phys. **11**, 131 (2015).

[37] M. B. Ruskai and F. H. Stillinger, Convexity inequalities for estimating free energy and relative entropy, J. Phys. A: Math. Gen. **23**, 2421 (1990).

[38] T. Sagawa, Second law-like inequalities with quantum relative entropy: An introduction, in *Lectures on Quantum Computing, Thermodynamics and Statistical Physics*, Kinki University Series on Quantum Computing Vol. 8, edited by M. Nakahara and S. Tanaka (World Scientific, Singapore, 2013), p. 127.

[39] M. Campisi, P. Talkner, and P. Hänggi, Fluctuation Theorem for Arbitrary Open Quantum Systems, Phys. Rev. Lett. **102**, 210401 (2009).

[40] M. Campisi, P. Talkner, and P. Hänggi, Thermodynamics and fluctuation theorems for a strongly coupled open quantum system: An exactly solvable case, J. Phys. A: Math. Theor. **42**, 392002 (2009).

[41] S. Deffner and E. Lutz, Generalized Clausius Inequality for Nonequilibrium Quantum Processes, Phys. Rev. Lett. **105**, 170402 (2010).

[42] V. B. Braginsky, Y. I. Vorontsov, and K. S. Thorne, Quantum nondemolition measurements, Science **209**, 547 (1980).

[43] C. P. Sun, X. X. Yi, S. R. Zhao, L. Zhang, and C. Wang, Dynamic realization of quantum measurements in a quantized stern - gerlach experiment, Quantum Semiclass. Opt.: J. Eur. Opt. Soc. B **9**, 119 (1997).

[44] E. Joos, in *Decoherence: Theoretical, Experimental, and Conceptual Problems*, Lecture Notes in Physics, Vol. 538. (Springer, Berlin, Heidelberg, 2000), pp. 1–17.

[45] W. T. Strunz, L. Diósi, and N. Gisin, Non-markovian quantum state diffusion and open system dynamics, in *Decoherence: Theoretical, Experimental, and Conceptual Problems*, Lecture Notes in Physics Vol. 538 (Springer, Berlin, Heidelberg, 2000), pp. 271–280.

[46] Q. A. Turchette, C. J. Myatt, B. E. King, C. A. Sackett, D. Kielpinski, W. M. Itano, C. Monroe, and D. J. Wineland, Decoherence and decay of motional quantum states of a trapped atom coupled to engineered reservoirs, Phys. Rev. A **62**, 053807 (2000).

[47] N. Hermanspahn, H. Häffner, H.-J. Kluge, W. Quint, S. Stahl, J. Verdú, and G. Werth, Observation of the Continuous Stern-Gerlach Effect on An Electron Bound in an Atomic Ion, Phys. Rev. Lett. **84**, 427 (2000).

[48] R. E. S. Polkinghorne and G. J. Milburn, Single-electron measurements with a micromechanical resonator, Phys. Rev. A **64**, 042318 (2001).

[49] W. H. Zurek, Decoherence and the transition from quantum to classical – revisited, Los Alamos Sci. **27**, 86 (2002), arXiv:quant-ph/0306072.

[50] M. Ballesteros, M. Fraas, J. Fröhlich, and B. Schubnel, Indirect acquisition of information in quantum mechanics, J. Stat. Phys. **162**, 924 (2016).

[51] B. D'Anjou, L. Kuret, L. Childress, and W. A. Coish, Maximal Adaptive-Decision Speedups in Quantum-State Readout, Phys. Rev. X **6**, 011017 (2016).

[52] J. Dalibard, Y. Castin, and K. Mølmer, Wave-Function Approach to Dissipative Processes in Quantum Optics, Phys. Rev. Lett. **68**, 580 (1992).

[53] H. J. Carmichael, Quantum Trajectory Theory for Cascaded Open Systems, Phys. Rev. Lett. **70**, 2273 (1993).

[54] E. A. Power, The natural line shape, in *Physics and Probability: Essays in Honor of Edwin T. Jaynes*, edited by W. T. Grandy, Jr. and P. W. Milonni (Cambridge University Press, Cambridge, England, 1993), pp. 101–112.

[55] E. T. Jaynes, Information theory and statistical mechanics. II, Phys. Rev. **108**, 171 (1957).

[56] L. D. Landau and E. M. Lifshitz, *Quantum Mechanics: Non-relativistic Theory* (Pergamon, Oxford, England, 1977), Chap. 6, p. 49.

[57] A. Shabani and D. A. Lidar, Completely positive post-markovian master equation via a measurement approach, Phys. Rev. A **71**, 020101 (2005).

[58] S. Maniscalco and F. Petruccione, Non-markovian dynamics of a qubit, Phys. Rev. A **73**, 012111 (2006).

[59] S. Haroche and J.-M. Raimond, *Exploring the Quantum: Atoms, Cavities, and Photons* (Oxford University Press, New York, 2006).

[60] H. Walther, B. T. H. Varcoe, B.-G. Englert, and T. Becker, Cavity quantum electrodynamics, Rep. Prog. Phys. **69**, 1325 (2006).

[61] S. Haroche, Nobel lecture: Controlling photons in a box and exploring the quantum to classical boundary, Rev. Mod. Phys. **85**, 1083 (2013).

[62] Note that the atom-field interaction should also contain a diamagnetic term that is ignored here but may sometimes be grouped with an effective change in ω_A [63].

[63] M. D. Crisp, Ed Jaynes' steak dinner problem II, in *Physics and Probability: Essays in Honor of Edwin T. Jaynes* (Ref. [54]), pp. 81–90.

[64] J. R. Johansson, P. D. Nation, and Franco Nori, QuTiP 2: A Python framework for the dynamics of open quantum systems, Comput. Phys. Commun. **184**, 1234 (2013).

[65] J. C. Wheeler, Nonequivalence of the nernst-simon and unattainability statements of the third law of thermodynamics, Phys. Rev. A **43**, 5289 (1991).

[66] P. T. Landsberg, A comment on nernst's theorem, J. Phys. A: Math. Gen. **22**, 139 (1989).

[67] Y. Rezek, P. Salamon, K. H. Hoffmann, and R. Kosloff, The quantum refrigerator: The quest for absolute zero, Europhys. Lett. **85**, 30008 (2009).

[68] R. S. Whitney, Thermodynamic and quantum bounds on nonlinear dc thermoelectric transport, Phys. Rev. B **87**, 115404 (2013).

[69] A. E. Allahverdyan, K. V. Hovhannisyan, D. Janzing, and G. Mahler, Thermodynamic limits of dynamic cooling, Phys. Rev. E **84**, 041109 (2011).

[70] E. T. Jaynes, Some aspects of maser theory, Microwave Laboratory Report No. 502, Stanford University, 1958.